

Lift Force on an Aerofoil

(lab experiment)

Jiaqi, Yao*

October 19, 2023

1 Outline

In this laboratory experiment, the focus is on determining the lift force acting on an airfoil using the Air Flow bench in a vertical wind tunnel. By examining the pressure distribution across the airfoil's surface at varying angles of attack, the experiment helps to relate these pressure to the overall lift produced by the airfoil.

2 Theory

Lift on an airfoil is important for aircraft elevation, which can be interpreted by the Coanda effect and the different pressures between top and bottom surfaces.

For a symmetric airfoil in zero angle, the lift generated is zero. After rising the angle of airfoil, the pressure variaty and producing more lift.

However, at significant angles, the airflow over the top of the wing can detach due to boundary layer effects, altering the pressure distribution and resulting in lower lift coefficients. This phenomenon is known as "stalling".

3 Method

- a. An accurate value for the density of air was determined using room temperature and atmospheric pressure, as cited in Rogers and Mayhew (1992 pp.157-8).
- b. With the aerofoil positioned at a 0° angle of attack, pressure measurements were recorded.
- c. The effective static pressure should be computed by using the atmospheric and duct inlet pressures.

*jy431@exeter.ac.uk

- d. Using the effective static pressure (p_{eff}) and the airbox pressure reading, calculate the free stream velocity and determined the Reynolds number with chord length.
- e. For each pressure tapping reading, the corresponding value of pressure ratio($C_{p,n}$) was calculated, and these values were plotted against ($\frac{x}{c}$). The curves were extended to represent a chord ratio of 0 and 1. Noticed that the pressure coefficient near the leading edge is approaching zero, which indicate the directing of the air is disappeared at this point. The exact position of this stagnation point changes with incident angle.
- f. From the generated curves of C_p , the lift coefficient (C_L) can be numerically integrated to derive its value.
- g. The measurements have been repeated for increasing angles of attack (in steps of 5°) up to 25° , with additional measurements at 17.5° and 22.5° . Following this, the lift coefficients were computed and a graph illustrating C_L vs. α for the aerofoil was plotted.

4 Results

The density of mercury and air and atmospheric pressure at this time can be determined from the thermometers (23.5°) and manometers ($754mmHg$).

The air and mercury densities are ($1.2kg/m^3$ and $13.534 \times 10^3kg/m^3$) and the atmospheric pressure is ($100107.4792Pa$), as shown by equation $P_a = \rho_{Hg}gh$ and by consulting the density - temperature table of mercury.

The following table shows the data recorded from the experiment.

5 Analysis

	1	3	5	7	9	11	2	4	6	8	10	12	Atm	Airbox	Inlet
0	196	158	152	158	167	177	184	156	155	164	170	182	186	244	190
5	236	195	175	175	178	182	124	118	132	148	168	180	186	244	192
10	146	220	197	187	188	187	58	88	106	146	164	180	186	244	194
15	244	235	212	199	194	189	13	54	116	146	166	178	186	244	198
17.5	242	239	217	203	196	190	8	42	119	148	165	178	186	244	200
20	247	236	217	205	197	190	156	154	154	153	154	158	186	244	210
22.5	248	238	220	209	200	192	164	162	162	160	160	162	186	244	214
25	247	242	226	217	205	196	172	170	169	168	164	164	186	246	218

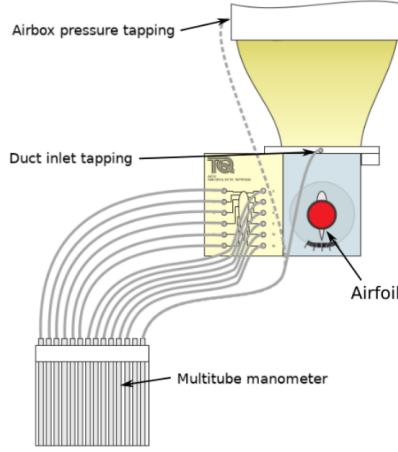


Figure 5.1: Pressure tappings for AF18 Experiment

Next the experimental data were processed. Firstly the difference in water head was calculated for each sampling point by using the Pitot tube at atmospheric pressure as a standard value. The difference in water head was then converted to a difference in pressure by equation $P_n = \rho gh$, as shown in table b below.

Based on the data, it was able to calculate the effective static pressure (p_{eff}) in different angle.

$$p_{eff} = p_0 + \frac{85}{135} \times (p_a - p_0) \quad (5.1)$$

And calculate free stream velocity U_∞ by following formular in different angle.

$$U_\infty = \sqrt{\frac{2 \times (p_{airbox} - p_{eff})}{\rho}} \quad (5.2)$$

The results are shown in the following table.

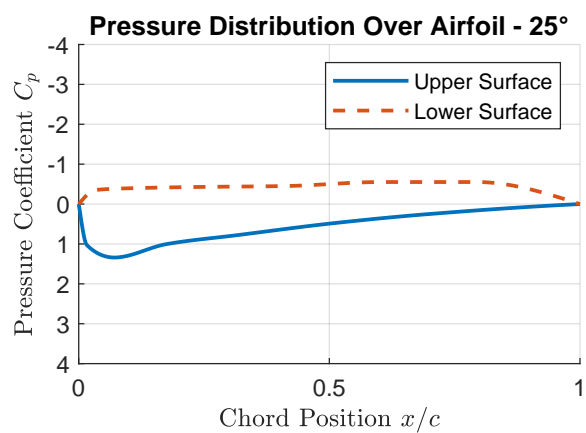
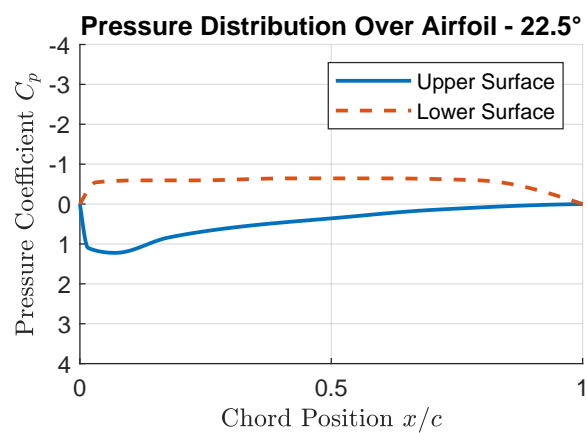
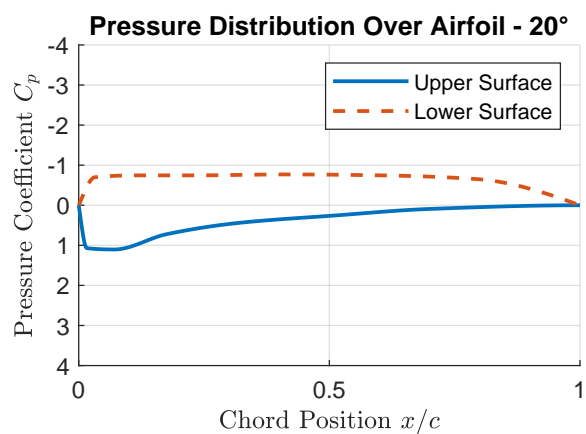
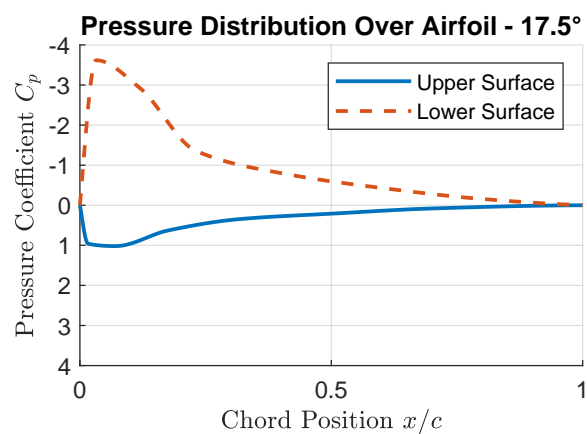
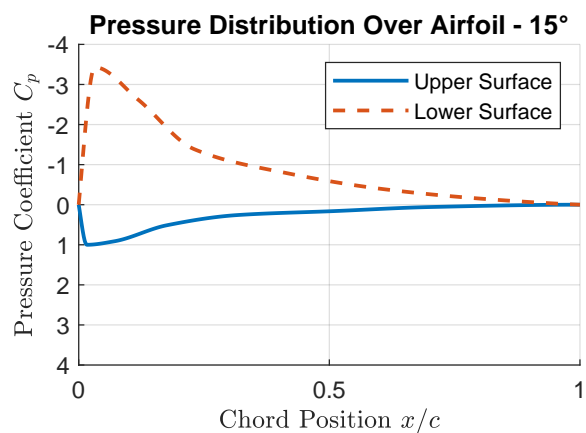
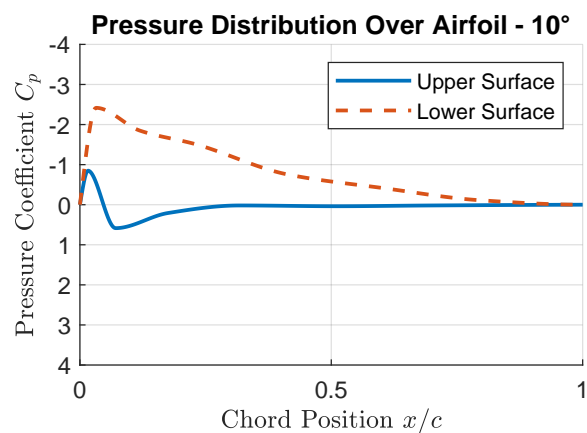
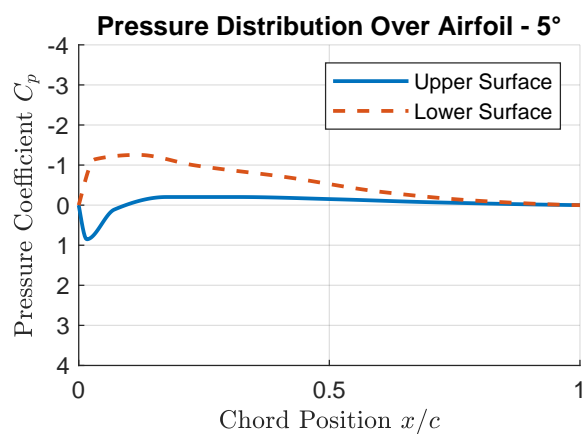
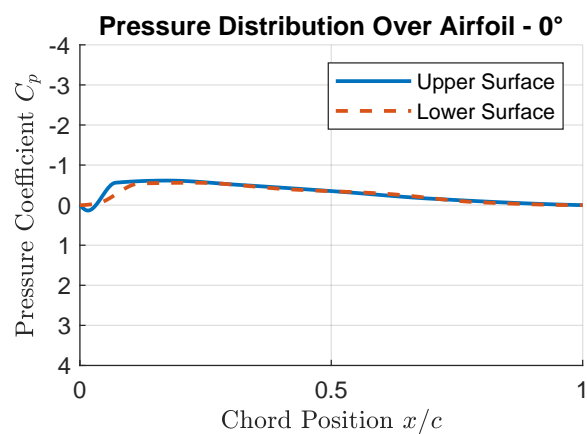
And from

$$C_{p,n} = \frac{p_n - p_{eff}}{\frac{1}{2} \rho u_\infty^2} \quad (5.3)$$

	1	3	5	7	9	11	2	4	6	8	10	12	Atm	Airbox	Inlet
0	98.1	-274.68	-333.54	-274.68	-186.39	-88.29	-19.62	-294.3	-304.11	-215.82	-156.96	-39.24	0	568.98	39.24
5	490.5	88.29	-107.91	-107.91	-78.48	-39.24	-608.22	-667.08	-529.74	-372.78	-176.58	-58.86	0	568.98	58.86
10	-392.4	333.54	107.91	9.81	19.62	9.81	-1255.68	-961.38	-784.8	-392.4	-215.82	-58.86	0	568.98	78.48
15	568.98	480.69	255.06	127.53	78.48	29.43	-1697.13	-1294.92	-686.7	-392.4	-196.2	-78.48	0	568.98	117.72
17.5	549.36	519.93	304.11	166.77	98.1	39.24	-1746.18	-1412.64	-657.27	-372.78	-206.01	-78.48	0	568.98	137.34
20	598.41	490.5	304.11	186.39	107.91	39.24	-294.3	-313.92	-313.92	-323.73	-313.92	-274.68	0	568.98	235.44
22.5	608.22	510.12	333.54	225.63	137.34	58.86	-215.82	-235.44	-235.44	-255.06	-255.06	-235.44	0	568.98	274.68
25	598.41	549.36	392.4	304.11	186.39	98.1	-137.34	-156.96	-166.77	-176.58	-215.82	-215.82	0	588.6	313.92

the pressure ratio in different angle can be calculated. Additionally, the tapping position and airfoil chord for the different sampling points can be obtained from the appendix, and the $\frac{x}{c}$ can be calculated.

Based on table a, Pressure distributions are plotted as a graph of the pressure ratio, which at 8 different angles with x/c as the x-axis and C_p as the y-axis.



	0	5	10	15	17.5	20	22.5	25
p_{eff}	24.70667	37.06	49.41333	74.12	86.47333	148.24	172.9467	197.6533
U_∞	30.11847	29.77471	29.42693	28.71875	28.35803	26.48081	25.69155	25.52602

	1	3	5	7	9	11	2	4	6	8	10	12
	0.016	0.071	0.175	0.317	0.510	0.698	0.032	0.119	0.230	0.413	0.603	0.794
0	0.135	-0.560	-0.613	-0.505	-0.342	-0.162	-0.036	-0.541	-0.559	-0.397	-0.288	-0.072
5	0.852	0.110	-0.203	-0.203	-0.148	-0.074	-1.143	-1.254	-0.996	-0.701	-0.332	-0.111
10	-0.850	0.585	0.208	0.019	0.038	0.019	-2.417	-1.850	-1.510	-0.755	-0.415	-0.113
15	1.000	0.913	0.515	0.258	0.159	0.059	-3.430	-2.617	-1.388	-0.793	-0.396	-0.159
17.5	0.959	1.019	0.630	0.346	0.203	0.081	-3.619	-2.928	-1.362	-0.773	-0.427	-0.163
20	1.070	1.103	0.723	0.443	0.256	0.093	-0.699	-0.746	-0.746	-0.769	-0.746	-0.653
22.5	1.099	1.223	0.842	0.570	0.347	0.149	-0.545	-0.594	-0.594	-0.644	-0.644	-0.594
25	1.025	1.340	1.004	0.778	0.477	0.251	-0.351	-0.401	-0.427	-0.452	-0.552	-0.552

By using the C_L formular, We can calculate lift coefficient C_L .

$$C_L = \frac{F_L}{\frac{1}{2}\rho U^2 A}$$

Noticed that A is the plan area of the aerofoil. By using mathematical method this can be evaluated by given equation:

$$C_L = \int \left[C_{pl} \left(\frac{x}{c} \right) - C_{pu} \left(\frac{x}{c} \right) \right] d \left(\frac{x}{c} \right)$$

However, an important point to note is that a direct integration requires a continuous function. In order to find the solution, we use discrete data points to evaluate the C_L by using **trapezoidal rule**. So, the discrete version of the integral becomes:

$$\Delta C_L = \sum \left(\frac{C_{pl,i+1} + C_{pl,i}}{2} - \frac{C_{pu,i+1} + C_{pu,i}}{2} \right) (x_{i+1} - x_i)$$

Where i is the index of the data points. The results show in a table below.

Degree	0	5	10	15	17.5	20	22.5	25
C_L	-0.040	0.383	0.676	0.939	1.015	0.840	0.828	0.830

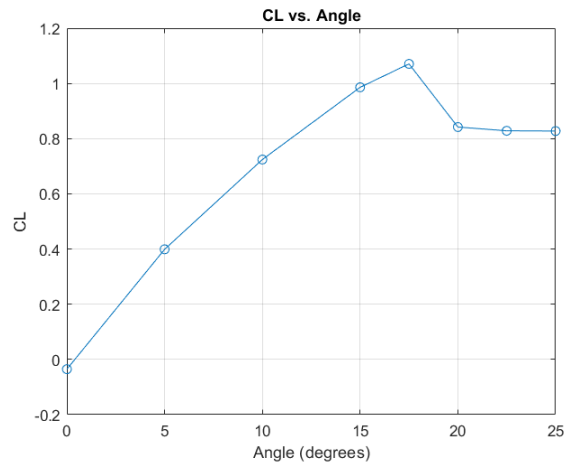


Figure 5.2: Experimental Demonstration

Error analysis

6 Conclusions

Based on the presented graphs, the pressure distribution over the airfoil for both the upper and lower surfaces demonstrates significant variations across different chord positions. The pressure coefficients on the upper surface tend to have more negative values as compared to the lower surface, indicating a higher velocity of flow and consequently a lower pressure. This is a fundamental concept in aerodynamics that contributes to lift generation.

Furthermore, the "CL vs. Angle" graph showcases the lift coefficient's relationship with the angle of attack. An initial increase in the lift coefficient is observed as the angle of attack rises. However, after reaching a peak, the lift coefficient appears to plateau or slightly decrease. This suggests that the airfoil reaches its optimal performance at a specific angle, after which increasing the angle does not yield additional lift and may even lead to stall conditions.

In conclusion, the pressure distribution patterns on the airfoil validate the principles of aerodynamics and the generation of lift. The relationship between lift coefficient and angle of attack is crucial in understanding the performance and efficiency of the airfoil, indicating the importance of optimizing the angle for maximum lift and avoiding angles that could lead to diminished performance or stalling.

References